

## **Response to the Reviewers and Editor**

The paper received very constructive and stimulating comments and suggestions from four Reviewers and the Editor. Thank you. There were two major points of critique that are the weak conclusion of maximization of entropy production in hydrology and the method of inference using power calculations and balances. Both points are due to the lack of theory that was obviously missing in the original manuscript, which is needed in the support of the novel ideas in my opinion and has been pointed out correctly by the reviewers. Note, some theory has been already touched upon in the detailed replies, but is still incomplete.

During my work on the revisions I realized that while the theory is tractable, the way of thinking of classic hydrologic problems in the context of entropy production and inference requires some serious adaptation. This is mainly due to the two-scale nature of the entropy balance equation constituting simultaneously a quite new perspective in hydrology, and potentially opening new ways for inference and upscaling in my opinion. Therefore, I decided to start with applications of the theory to the most basic hydrologic profiles with steady state and also transient groundwater flow, which is useful in the aforementioned adaptation process. And it turns out that new equations arise that, for example, relate the microscopic entropy production with an effective conductance coefficient connecting the flow with the force at the macroscale, which I call the method of inference from entropy balance considerations.

In my opinion, this study and the results constitute a full research paper proposing a new method and providing new insights into hydrology from a thermodynamic perspective. Therefore the topic of maximization of entropy production was removed from this manuscript and committed to a separate study in order not to confuse the reader.

## **Response to the Reviewers**

In the following, comments by Referee#1 are indicated with [R#1] in italic and replies by the author are indicated by [K].

[R#1] *The MEP principle is applied to a synthetic hillslope based on a spatially-distributed and physics-based model. The entropy production is computed. The research question is important and interesting. The methodology is reasonable. I have a few major comments related to the design of the simulation experiments. I hope my comments are useful for the authors to revise the manuscript.*

[K] I would like to thank the reviewer for the constructive comments, questions and suggestions, which help to improve the manuscript.

[R#1] *Lines 25-27 on Page 5127: Rainfall and other climatic variables (such as temperature and humidity) may be correlated. If rainfall is reduced by about 30% but other variables are not changed, this may be not realistic. Why not obtain the climatic data from a semi-arid watershed?*

[K] It is correct that rainfall and other climatic variables may be correlated. In the simulations, reducing the rainfall was a pragmatic approach in order to facilitate additional simulations in future with increasing rainfall that are consistent with the current setup in order to interrogate the results for different ratios of saturated hydraulic conductivity and rainfall rates  $K_{sat}/PCP$ . I feel this is reasonable given the large uncertainty of hourly rainfall, which may result in similar climate variable combinations, which were used in the simulations and which are reasonable in my opinion. (No rainfall was generated at time steps originally without rainfall.)

[R#1] *Related to the comment above: "Runoff out of the domain occurred only for  $K_{sat} = 0.0005 \text{ (m h}^{-1}\text{)}$  and S2 and was only 2.2 % of the annual precipitation." (lines 7-8 on page 5129). Even though for the case of runoff ( $Q$ )=2.2% of the annual precipitation ( $R$ ) → the ratio of annual evaporation ( $E$ ) to precipitation,  $E/PCP=0.98$  → according to Budyko curve,  $Ep/PCP > 3$  → potential evaporation  $Ep > 1900 \text{ mm}$  since  $R=637 \text{ mm}$  (line 1 on page 5128). I am not sure whether the setting of climatic variables can reach this potential evaporation (temperature is 291 K, line 27 on page 5127). It may be better to constrain the system to the observed pattern or reality when the MEP principle is used for understanding the system.*

[K] The climatic variables were obtained from the North American Regional Reanalysis Data Set for the water year 1998/1999 over Oklahoma and were used in previous studies (e.g. Kollet et al., 2008), which resulted in reasonable evapotranspiration checked against Ameriflux tower data. (The calculation of bare soil evaporation, which is relevant for presented study, is addressed in detail below.) Note, that in the aforementioned simulation case, runoff was produced by excess infiltration due to the local, random heterogeneity at the outlet of the hillslope at the "microscopic" scale. Different random realizations may not produce any excess infiltration runoff at all. Because the Budyko concept is valid at the watershed scale, I am not sure about its direct applicability to the hillslope simulations presented here. Yet it is correct that  $Ep \sim 1900 \text{ mm}$  would be high, but not completely unrealistic in my opinion. Large  $Ep/PCP$  ratios may also be linked to the thermodynamic equilibrium assumption, which is inherent in the calculation of bare soil evaporation in the simulation explained and discussed below.

In the context of the Budyko concept, I feel it is remarkable that the simulations actually demonstrate that a system can be sustained at dynamic equilibrium along the arid, water limited envelope curve ( $Ep/PCP > 1$ ) including a saturated zone. This is only possible, because of the non-linearity of variably saturated flow.

[R#1] *A further comment based on the above comments, how is evaporation determined?  $PCP=E$  for most of the cases. In these cases, the competition between evaporation and runoff is*

removed. "...entropy production inside equals the net entropy exchange with the outside." (Lines 3-5 on page 2125). How is the power by the evaporation process related to the power computed in this paper? Maximum entropy production (or power) principle is used for a particular flux, and the conductance coefficient is treated as the decision variable. From the system perspective, the entropy production by all the fluxes such as discharge and evaporation may need to be summed (Wang et al., 2015, DOI: 10.1002/2014WR016857). There are two types of competition or tradeoff in the system: 1) flux and gradient for a particular flux; 2) among different types of fluxes (e.g., evaporation versus runoff). In this paper, some of competitions (e.g., runoff and evaporation) is pre-defined. Some discussions and clarifications will potentially be valuable for the readers.

[K] In the simulations, the variably saturated groundwater-surface water flow model ParFlow (PF) coupled to the land surface model CLM (Common Land Model) was used. PF calculates variably saturated flow based on Richards equations in a continuum approach, and surface runoff based on a free surface overland flow boundary condition. CLM calculates the water and energy balance i.e. the exchange of moisture and energy (including evaporation from the bare soil,  $E$ ) with the atmosphere based on the Monin-Obhukov similarity principle. Thus,  $E$  is calculated based on

$$E = -\frac{\rho_{atm}}{r_{aw}}(q_{atm} - q_s)$$

where  $\rho_{atm}$  is the density of the atmosphere;  $r_{aw}$  is an exchange functional explained below; and  $q_{atm}$  and  $q_s$  are the atmospheric and soil specific humidities, respectively.

The exchange functional  $r_{aw}$  is determined by turbulence generated mechanically (based on the logarithmic wind profile) and by buoyancy forces, and is thus a function of the stability of the atmosphere and must be determined iteratively. The atmospheric specific humidity  $q_{atm}$  is provided by the atmospheric forcing time series and  $q_g$  is calculated using Kelvin's equation, which includes the soil matric potential. The latter constitutes an important coupling of variably saturated subsurface flow with the evaporation and is handled in an operator splitting approach in PF.CLM: at each time step, PF calculates the moisture redistribution based on the evaporative sinks provided by CLM in the top model layer; then the matric potential values are passed to CLM, which in turn are used to calculate the moisture dependent energy fluxes including  $E$ . Thus, neither evaporation nor the top boundary condition for subsurface soil moisture redistribution or runoff is pre-defined. They all interact freely based on the coupling, which is key in the entropy production considerations. This is also the reason why decades of spinup simulations need to be performed until the system reaches a dynamic equilibrium. It is important to mention that the application of Kelvin's equation is based on the assumption of thermodynamic equilibrium and may lead to a positive bias in bare soil evaporation estimates, when compared to measurements. This may also be the case here, however, it is not the goal to reproduce measurements, but incorporate important couplings and represent realistically the important degrees of freedom of the subsurface coupled to the land surface.

The power budget is performed for the subsurface, where the power due to evaporation is related to sinks in the top model as explained above. The sinks produce gradients and fluxes toward the top model layer producing power, which were calculated locally using equation 7 through 9 and including the local power budget given by equation 10. Equivalently, precipitation produces gradients and fluxes away from the top model layer producing power, which was calculated in the same way. In that way all the fluxes producing power were summed. At dynamic equilibrium, the *global* power budget was closed to an increment of  $10^{-12}$  to  $10^{-14}$   $\text{m}^2\text{a}^{-1}$ !

While globally (over the entire hillslope)  $PCP = E$ , there is still competition between the net flux  $q$  (entering along the recharge zone as  $q^{inf}$  and leaving along the discharge zone as  $q^{ex}$ ), evaporation, and the dynamic water table. This competition results in the maximization of entropy production in the recharge/discharge zone. It is true that net entropy production over the *entire* domain is zero given that  $PCP=E$ , however there is net entropy export in the recharge zone because of  $q^{inf}$  and net entropy import in the discharge zone because of  $q^{ex}$ .

In addition to the explanation of the summation of all fluxes, it is important to re-emphasize the difference between the useful approach outlined in Wang et al., 2015, DOI: 10.1002/2014WR016857 and the presented study. Wang et al. already work at the macroscopic scale assuming that there exists a representative macroscopic soil chemical potential  $\mu_s$  and effective transfer coefficient,  $k_e$ , for the soil-land surface flux (in their case vegetation flux). In the presented study, a "microscopic" point of view is taken in which the nonlinear fluxes, gradients and interactions with evaporation evolve freely, without any constraint or predefined decision variable. Note that competitions are *not* predefined. Simulating the actual "microscopic" process the study shows that entropy production maximization occurs at the macroscopic level out of the non-linear processes. In addition, an approach is suggested to arrive at a macroscopic soil chemical potential and effective exchange coefficient as it is used in Wang et al.

[R#1] Lines 11-13 on Page 5128: *No flux cross the vertical boundary at  $x=0$ ? Why not set free discharge at the boundary of  $x=0$  and assuming negligible water depth in the channel?*

[K] The hillslope can discharge freely at the top at  $x=0$  based on the free surface overland flow boundary condition and zero depth gradient condition.

[R#1] Line 17 on Page 5128: *"In order to identify"*  
Equation (4) on page 5129 and other places: *the superscript of net exfiltration/infiltration is changed to (-ex, inf)?*

[K] This will be reconciled in the revised manuscript.

## References

Kollet SJ, RM Maxwell, 2008, Capturing the influence of groundwater dynamics on land surface processes using an integrated, distributed watershed model. Water Resour Res. 44 (2), Doi 10.1029/2007wr006004.



In the following, comments by Referee#2 are indicated with [R#2] and replies by the author are indicated by [K].

[R#2] *This paper applies the maximum entropy production (or maximum power) principle to a relative simple model of the unsaturated zone. It determines the power in each grid cell of which the spatiotemporal mean is taken. This is done for different values of  $K_{sat}$  and it appears that two maxima in power exist. Subsequently, a conceptual model is described and from the spatiotemporal mean of the fluxes and of power an effective conductance is calculated. Interestingly, the two optimum values of  $K_{sat}$  collapse into a single value of the effective conductance. Both analyses are done for a case of homogeneous  $K_{sat}$  and a heterogeneous  $K_{sat}$  field. This is an interesting paper and eventually worth publishing. However, some more clarification and rewriting are needed before that.*

[K] I would like to thank the reviewer for the constructive comments, questions and suggestions, which help to improve the manuscript.

[R#2] *For example, I was especially confused by the conceptual model (Fig. 5). This model is presented as being the same model as in Kleidon and Schymanski (2008) and Westhoff et al. (2014). However, in their models there is competition between runoff and evaporation which is missing in Fig. 5. But I was even more confused, because Kleidon and Schymanski (2008) and Westhoff et al. (2014) optimized their conductance within the framework of their model, where for each value of the conductance the power is calculated. In this paper, the maximum power principle is used to come to a macroscopic head difference and a macroscopic conductance that can replace the microscopic heads and the microscopic  $K(\theta)$ . This is a completely different methodology to get the macroscopic parameters. I suggest to better communicate this in the revised version.*

[K] In my opinion, the conceptual model is the same as in Kleidon and Schymanski (2008) and Westhoff et al. (2014). In the presented study, there is competition between the net flux (between the recharge and discharge zone) and evaporation, equivalent to the competition between runoff and evaporation in e.g. Westhoff et al. (2014). Note, neither the net flux nor evaporation are prescribed in the simulations; both are a function of the non-linear hydrodynamics of variably saturated flow, and the reciprocal, nonlinear dependence of evaporation on the moisture state of the shallow subsurface and the atmospheric forcing. This has been discussed in the reply to Referee#1 and will be repeated below for completeness.

The conceptual model is perhaps better reflected in the figure A below with a connected, dual bucket model, which may replace figure 5 in the revised manuscript. Here, the recharge and discharge zones are represented with buckets having a high and low hydraulic head  $H_h$  and  $H_l$ , which are connected through an interface with a conductance  $\lambda_{eff}$ .

I agree that the proposed methodology is completely different, because no fluxes, etc. are prescribed in the microscopic simulations, which lead to maximization of power purely from the non-linear competition between variably saturated subsurface flow and evaporation driven by an atmospheric time series.

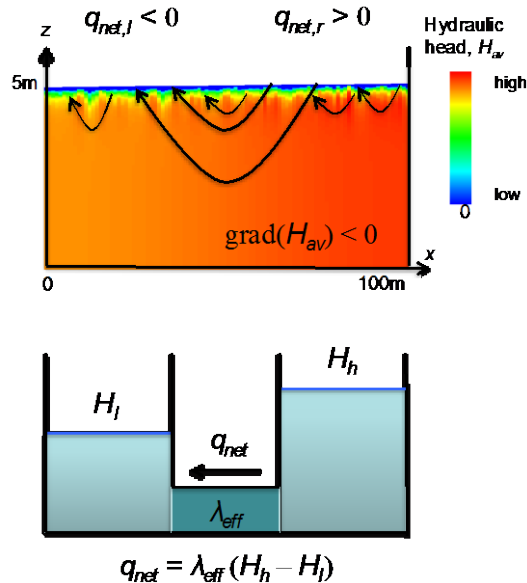


Figure A. Conceptual approximation of the "microscopic" hillslope model with a connected, dual bucket model.

[R#2] Besides this I also miss a verification of the macroscopic model: Once the optimum macroscopic parameters have been defined, run the macroscopic model with the same climatic forcing as the microscopic model and compare the resulting fluxes with the microscopic model. This may also shed more light on the fact that two optima of  $K_{sat}$  collapse into one optima in  $\lambda$  (why this happens is still unclear to me).

[K] The macroscopic model is macroscopic in space and time at dynamic equilibrium. Non-linear variability can not be resolved. Thus, it can not be applied to the hourly climate forcing and simply be validated with the microscopic model. At this point the goal was to suggest a methodology to arrive at a macroscopic model including a macroscopic force, which is otherwise unseizable. However, at this point, it is not clear how to validate this macroscopic force or effective conductance coefficient, because both are not measurable quantities. The results shown in figure 7 suggest that the mean hydraulic head at the bottom of the flow domain, which can be measured in the field, may be a good indicator of the effective state of conductance. Similar indicators are required for the effective force in order to ultimately validated the macroscopic model and make the model useful for predictions in future.

The collapse of the  $K_{sat}$  into one optima in  $\lambda$  is due to the fact that the effective exchange coefficient does not increase monotonously with  $K_{sat}$  (figure 6b). The conductance of the macroscopic system decreases as soon as the groundwater reservoir falls dry (grey area in figure 6a). This is to the nonlinear dependence of the relative permeability on the degree of saturation, which is described by the van Genuchten relationship in the model.

[R#2] P5127, L25: add a graph with time series of the forcing

[K] The atmospheric time series consists of 8 forcing variables (long-/shortwave radiation, precipitation, air temperature, 2 wind speed components, specific humidity, barometric pressure). The plot will be provided in the revised manuscript containing exemplarily time series of precipitation and air temperature.

[R#2] *P5131, Eq. 10 and 11: Power cannot be summed. Instead the mean should be taken, so it should be divided by NT and NK.*

[K] This will be reconciled in the revised manuscript.

[R#2] *P5132, L7-13: To make this point clearer, I suggest adding a similar figure as Fig.1 but than for a dry and a wet period in time.*

[K] This will be included in the revised manuscript.

[R#2] *P5133, L1: The zone of net inflow is not necessary a net exporter of power. Rephrase to 'incoming water produces more power than outgoing water' or 'incoming fluxes are driven by larger gradients than outgoing fluxes P5133, L3: Are the different zones related to the part they cover at the pf-curves (e.g. convex or concave parts of the curve)?*

[K] This will be rephrased.

[R#2] *P5133, L22-23: If the cross-section is taken a little bit to the right or left, the P values will be much larger in the groundwater reservoir.*

[K] This is correct, but the general shape will be very similar or the same.

[R#2] *P5133, L27: Why does the spatiotemporal mean darcy flux change with changing Ksat? The input (rainfall) and output (evaporation) of water is fixed, so the total mean flux should remain constant.*

[K] Because the mean Darcy flux is function of the Ksat at dynamic equilibrium.

[R#2] *P5135, L20- P5136, L3: I suggest to move this part to the introduction, since it explains the objective of the paper much better than currently.*

[K] This is a good suggestion and will be revised.

[R#2] *P5137, L11-14: I don't understand this explanation*



[K] Lambda does not increase monotonically with Ksat. When the groundwater reservoir falls dry lambda decreases with increasing Ksat.

[R#2] P5138, L1-7: *I don't understand this part. Please be more specific: e.g. to which subfigures are you referring? Do you mean that the slope of lambda in increasing monotonously?*

[K] Here I was trying to explain which effective parameter is responsible for the maximum in the power. The explanation will be revised with clear references to the different subfigures.

[R#2] P5140, L4: *Power can indeed not be measured directly, but suction heads and  $K(\theta)$  can. With this, power can be calculated (although I recognize that these observations are point measurements, while in real hillslopes macropores are also present)*

[K] This is correct, but validation with point measurements will be very difficult.

[R#2] Fig. 3: *Indicate in Fig. 2 which cross-section is taken for this figure.*

[K] This will be done in the revised manuscript.

[R#2] P5126, L18: *Two maxima in power were found, but for different conductance values (and unique climatic forcing)*

[K] Will be corrected in the revised manuscript.

[R#2] P5127, L20: *If PF.CLM provides evaporation, than net radiation, sensible heat and ground heat fluxes are not needed for this exercise.*

[K] CLM calculates iteratively evaporation based on closing the energy balance  $R_{net} = LH + H + G$ . Therefore the energy fluxes are needed.

[R#2] P5128, L6: *remove the percentage sign?*

[K] Will be reconciled in the revised manuscript.

[R#2] P5128, L12: *'and of... at the top': rephrase*

[K] Will be rephrased in the revised manuscript.

[R#2] *P5129, L12: PCP: keep to the conventions of HESS: Variables consist of one letter/symbol and the rest in sub- or superscript (applies also to other variables)*

[K] Will be corrected in the revised manuscript.

[R#2] *P5129, Eq. 4: add the overflow terms*

[K] Correct, they will be added in the revised manuscript.

[R#2] *P5133, L8-9: The stair-step like representation can also be seen as a numerical artefact.*

[K] It is a numerical artifact in the sense that it is a result of the finite difference approximation in the realm of discrete mathematics.

[R#2] *P5134, L26: What is meant by 'correct location'?*

[K] More data points are needed with respect to different  $K_{sat}$  to resolve the discontinuity more accurately.

[R#2] *P5136, L24: the maximum at  $\log(K_{sat}) = -3$  is difficult to see in Fig. 6a. It rather seems to have a maximum at the edge of the parameter space.*

[K] I checked the values again and the maximum is located at  $\log(K_{sat}) = -3$ .

[R#2] *P5138, L9-10: please rephrase. There exist a maximum in power in the MATHEMATICAL model of the hillslope.*

[K] Will be rephrased in the revised manuscript.

[R#2] *Fig 1: Indicate that blue is relatively dry and red is wet (or use a logarithmic scale).*

[K] This will be revised.

## References

Schymanski, S. J., Kleidon, A., Stieglitz, M., and Narula, J.: Maximum entropy production allows 10 a simple representation of heterogeneity in semiarid ecosystems, *Philos. T. R. Soc. B*, 365, 1449–1455, doi:10.1098/Rstb.2009.0309, 2010.

In the following, comments by Referee E. Zehe are indicated with [Z] and replies by the author are indicated by [K].

[Z] *This study examines free energy conversions associated with subsurface water flows within numerical experiments at a synthetic hillslope. More specifically the author perturbed saturated hydraulic conductivity for a given set of soil hydraulic parameters in search for an optimum value maximizing entropy production/power in subsurface flows and elaborates on the role of the groundwater surface and on the role of purely random heterogeneity in this context. Furthermore, the author proposes an interesting approach how to use MEP for inferring/upscaling functional optimum, effective subsurface water characteristics within larger control volumes. Particularly, the last point is interesting and novel. The proposed study is, hence, without of high potential interest for HESS.*

*Nevertheless, I got the imprecision that the study is compiled a little too hastily, which is partly reflected in superficial referencing (as explained below) and the too narrow range of properties that is investigated within the experiments. The study would greatly from a thorough revision a) to improve physical rigor in the proposed approach how to estimate “power” within the model domain and to broaden the type and range of terrestrial controls on subsurface water flows and related free energy dissipation within the numerical experiments.*

[K] I would like to thank the reviewer for the constructive comments, questions and suggestions, which help to improve the manuscript. The points raised above also with respect to physical rigor and broadening the range of terrestrial controls will be addresses below and in detail in the revised manuscript.

[Z] *I encourage the author, for whom I have high respect, to further optimize this potentially very interesting study by addressing the following points:*

*Major point concerning referencing:*

- *I appreciate the authors effort to refer to recent studies dealing with thermodynamic optimality in hydrology (some of those I authored/co-authored myself). The way how these studies are discussed is, however, not appropriate. After reading the introduction, one is left with the imprecision that this is the first study using “physics-based” models instead of bucket models shed light on the role of MEP in hydrology. This is not quite the case, for instance: o Porada et al. (2011) used a 1d-implementation of the Richards equation combined with a SVAT-approach and showed for the 35 largest catchments in the world, that the MEP optimized configuration plotted in a short envelope around the Budyko curve.
  - o Zehe et al. (2013) used a 2-d Richards-model (coupled with a SVAT and 1 d overland flow) within numerical experiments exploring free energy conversions and dissipation associated with subsurface water flows and different runoff components. More specifically we perturbed the flow resistance in hillslope scale models and found the those values which optimize steady state production of entropy (or equivalently the reduction of free energy), perform acceptable in predicting rainfall runoff behavior two different catchment.*

- *Kleidon and Renner (2013) proposed a simple model (based on three parameters) to predict land surface energy exchange based on the idea of maximizing power in the virtual and sensible heat flux and that the sensible heat flux operates at the Carnot limit. The model performs strikingly well when being compared against flux tower data in different land use settings during convective conditions.*

*I very much agree that “physics based” models are superior for exploring to which extent thermodynamic optimality indeed applies; however, it is a matter of fairness to acknowledge that this has been addressed by the reported studies. Maybe the formulation PDE based or hyper resolution models is more appropriate as physics-based, as it does not imply the other models are not based on physics.*

[K] I do not want to leave the impression of unfairness. I am very much aware of the aforementioned studies, which are of deep interest to me and contribute truly novel ideas to hydrology. By physics based and as a difference to previous studies I meant that Richards equation is applied at the support scale, and production of entropy is calculate at this scale as it is suggested by the theory in my opinion. To illustrate this, following Kondepudi and Prigogine 1998, the entropy balance equation is

$$\frac{\partial \mathbf{s}}{\partial t} + \nabla \cdot \mathbf{J}_s = \sigma \quad (\text{i})$$

where the first term on the left hand side is the temporal entropy change; the second term on the left hand side is the divergence of the entropy current (entropy that enters/leaves the macroscopic domain); and  $\sigma$  is internal entropy production due to sum of all internal, "microscopic" forces,  $F_i$ , and fluxes,  $J_i$ , defined as

$$\sigma = \sum_i F_i J_i \quad (\text{ii})$$

In the simulations, the entropy production was calculated directly at the support scale by summation of all local forces and fluxes. The term power was used because temperature does not change. However, this is inappropriate, because generation of power is simply neglected; it is the microscopic dissipation of the gradients by the fluxes in (ii), which produces the entropy as pointed out by the Referee. Additional thoughts on equation (i) and (ii) will be provided below, which will lead to a reanalysis of the simulation results and clarifications in the revised manuscript.

[Z] *Major scientific points:*

*The author propose essentially to calculate power based on in- and outward soil water fluxes into the model grid elements and local gradients, to summarize these values over time and then compile the spatial integral. With this he adopts a macroscale formulation of power (usually employed at the system scale using fluxes across the boundaries and macroscale gradients) which applies for steady states in gradients and fluxes to the microscale. This is due to several reasons inappropriate because the grid scale gradients get depleted by the fluxes within a simulation time step means there is no steady state.*

[K] In the simulations, conditions of dynamic equilibrium were produced i.e. the simulation year was run repeatedly with identical hourly atmospheric forcing until the water balance and entropy ( $ds/dt=0$ ) over the simulation year did not change. This required more than 30 years (in some of the heterogeneous cases 60 years) of simulation! The only assumption in equation (i) is that the system is not far from equilibrium, which is the case in the simulations. Thus, applying equation (i) to instantaneous fluxes and gradients while including all required components in the divergence of the entropy current is appropriate in my opinion and results in  $ds/dt = 0$  over one full cycle at dynamic equilibrium i.e. the statistical steady state. This is discussed again below.

[Z] *Secondly, soil water fluxes are essentially dissipative by their nature (pushing the system back to local thermodynamic equilibrium) and kinetic energy associated with soil water fluxes is marginal (this where power could be extracted from to perform work). The calculated term is thus not power (a source term in the free energy balance) but dissipation (the sink term in the free energy balance). As eq. 10 deals in fact dealing with dissipation, the proposed summation in is hence not appropriate, as positive and negative terms cancel out. (The latter wouldn't harm when dealing with a system conserving free energy, which does not perform work when traveling along a closed path). One can think about a case where all summands in Eq. 10 cancel, the equations suggests that nothing happened at all; although gradients have been depleted and re-established many, many times and which implies dissipation of energy. Maybe, the way to go is to multiply the net flux into a local grid element with temporal change in the local potential (see post discussion of Zehe et al. 2013 for the details) or to use the method proposed in Zehe et al. (2013).*

[K] The Referee is correct that the theory and analysis needs to be clarified. It was intended to integrate the equation (i) over the dynamic equilibrium of one cycle/year by calculating the total entropy production, which equals the divergence of the entropy current, because  $ds/dt = 0$  over one full cycle i.e. one complete simulation year. Thus, it is correct that there is entropy production (dissipation) even if the net flux is zero. This and additional implications can be illustrated in a simple thought experiment: removing the topographic slope from the synthetic hillslope experiment results in a bucket which is closed laterally and at the bottom, and is in contact with the atmosphere at the top. Performing the same dynamic equilibrium simulations as before will result in a net or mean flux of zero over one full cycle (because the bucket can not dry out infinitely). Because of the fluctuations in the flux there will be dissipation and entropy production. Thus,  $ds/dt = 0$  over one full cycle; and the internal entropy production integrated over one full cycle equals the divergence of the entropy current integrated over one full cycle. However, the divergence of the entropy current now consists of the exchange with the outside via the top boundary (evaporation/infiltration) and the internal, local fluctuations close to equilibrium, which may be understood as local (entropy) sinks/sources. Thus, in the analysis these fluctuations need to be included. To check this I integrated

$$\nabla \cdot \mathbf{J}_s = \frac{\mu}{T} (\nabla \cdot \mathbf{q}) \quad (\text{iii})$$

and

$$\sigma = \sum_i F_i q_i \quad (iv)$$

$$F = -\nabla \frac{\mu}{T}$$

over one full cycle over the hillslope for one example of  $K_{sat} = 0.01$  m/h (where  $\mu$  is the chemical potential, in this case the hydraulic head; and  $T$  is temperature, in this case constant), which yields an absolute difference of  $-5.53 \times 10^{-10}$  m<sup>2</sup>/a, which is on the order of  $10^{-15}\%$  of the total entropy production. This tells me that the system is entropy conservative and equation (i) is applicable at dynamic equilibrium.

[Z] *The authors needs to show that his analysis reflects steady state behavior by compiling longer simulations using a longer time series reflecting the more than one year of forcing conditions.*

[K] Dynamic equilibrium (statistical steady state) over one full cycle/year is the prerequisite of the proposed method and was ensured with multiple decades of spinup simulation.

[Z] *I d' like to encourage the author to better link the numerical experiment to natural systems and to explore a wider range in natural controls. The proposed simulation domain has, expect of a very small and homogeneous topographic gradient, not much in common with a natural hillslope. Also the soil should be better characterized than just dropping the van Genuchten-Mualem parameters (similarly the boundary conditions). Even when the author prefers not to deal with transpiration, it is straight forward to compare for instance fine and coarse porous soils (with different importance of capillary pressure in this concert), different topographic gradients (to come closer to a hillslope) and eventually forms.*

[K] The constructive suggestions by the Referee are very well received. A direct link to natural systems is the ultimately goal including the demonstration of the predictive capability of the methodology. Also major aspects raised by the Referee such geometry of the hillslope, soil characterization, boundary conditions, and additional processes such as transpiration need to be addressed. However, this is beyond the scope of a single study, because of the required compute time of the hyper resolution simulations for dynamic equilibrium and extremely large set of potential simulations. The scope of the study is to propose a new methodology supported by, at this point, synthetic hillslope experiments.

[Z] *The reported dependence that purely random heterogeneity in ksats yields to an elevated maximum in dissipation is by far too interesting, to treat it in such a brief manner. How does this depend on the variance of ksats (which I missed by the way in the manuscript)? How does this change when adding a spatial co-variance? Is it a steady decrease within increasing correlation length, or is there a maximum dependent on the correlation length? This is particularly interesting as correlation lengths in natural soils are short (several meters).*

[K] This appears to be indeed the case, but must be corroborated in the revised analysis. Following the discussion above, entropy production may increase with random heterogeneity, because of an increase in the fluctuations of the flux and perhaps also because of an increase in the mean flux. Again, there is an extremely large set of simulations required in order to interrogate the impact of e.g. spatial structure at different scales. In the revised manuscript, additional results will be provided for different variances of the random distribution.

[Z] *The last part dealing with MEP as an inference principle and the suggested approach to estimate a macroscopic gradient and conductance is for me the most interesting part of the study. However, the provide evidence does support the conclusion that MEP applies indeed to hydrological system in the sense that an optimized effective conductance performs well against observations. This implies a) to show that optimum hillslope structure have predictive power against data and that the up-scaled effective conductance works well when being used within a water balance simulations carried out at larger grid cells (as for instance shown by Lee et al. 2007). Westhoff and Zehe (2013) showed that MEP is not useful for conceptual modelling, as the optimum parameters had not predictive power for the water balance; Zehe et al. (2013) reports to 2 successful cases, which can be just a coincidence). So there is still room for more evidence here.*

[K] The Referee is correct that the demonstration of the predictive power against data and in water balance simulations at larger grid cells is lacking. At this point, it is not clear how to provide evidence, because the relationships provided so far are for a limited set of synthetic cases. More simulations and application to a natural hillslope are planned in future but are out of the scope of this study in my opinion.

[Z] *Please not that Eq. 1 is only valid, in case of mass flows, which are driven by chemical potentials and during steady states.*

[K] Please see my replies with regard to equation (i).

[Z] *Power is as a flux an intensive property and can thus not be imported/exported or balanced. Please refer to in/export of free energy which is an additive quantity.*

[K] This will be clarified in the revised manuscript following also the discussion above. The entropy balance including fluctuations will be revised.

[Z] *Hourly differences of P-ET are not equal to infiltration but equal to infiltration and surface runoff (Eq. 4). Why not using the influx into the model domain?*

[K] Correct, surface runoff will be added to the equation.

[Z] *How does the model deal with the saturated zone- in an iterative manner allowing for a free surface or by using storage coefficients?*

[K] Richards equation is applied in a continuum approach including the saturated and variably saturated zone allowing for a free surface (water table).

[Z] *Is it not really astonishing, that a saturated domain builds up as you use a no flow boundary?*

[K] The domain could be infinitely deep and there still would be a water table, which is purely the result of the interaction of non-linear, variably saturated flow and evaporation/infiltration at the top based on the atmospheric forcing time series.

[Z] *Page 5131 typo: toward by towards*

[K] Will be corrected in the revised manuscript.

[Z] *The gradient should point into the opposite direction of the flux (which reflects the second law of thermodynamics) not into direction of the flux*

[K] This will be corrected.

[Z] *Maybe replace small scale chaos with small scale disorder*

[K] This suggestion will be honored.



In the following, comments by Referee S. Schymanski are indicated with [S] and replies by the author are indicated by [K].

[S] *The paper contains a range of interesting results and discussion, but I believe that the insights with respect to maximum entropy production or power presented in this study could be enhanced a lot and need some clarifications. I also found some potential flaws that need to be dealt with.*

[K] I would like to thank the reviewer for the constructive comments, questions and suggestions, which help to improve the manuscript.

[S] *First of all, the author did not explain how water fluxes are calculated in the model, whether hydraulic heads used for calculation of entropy production include gravitational potential and how fluxes out of the domain were modelled.*

[K] In the model, the fluxes are calculated based on Richards equation. Entropy production calculations are based on hydraulic head, which includes the gravitational potential per definition. Fluxes in and out of the domain are modeled as sources and sinks that come from the coupling with CLM. This will be elaborated in detail in the revised manuscript.

[S] *Power (representative of entropy production) is only calculated for internal flow processes, no calculation of entropy exchange between grid cells or for water exchange across the boundaries is presented. As the author points out on P. 5126 L1, entropy production or power is a positive quantity by definition, so I am uncertain how to interpret Fig. 2 with positive and negative values of average net power. In fact, the big red block with sharp boundaries in Fig. 2a looks like an artefact to me and should be analysed/discussed in more detail. At steady state, entropy in each grid cell must be constant, meaning that the entropy produced internally must equal the net export of entropy to the surroundings Schymanski et al. (2010). For a dynamic steady state, as assumed in the present paper, this must be true for long-term average entropy balance, so I believe that a detailed calculation of the entropy balance, not only entropy production, may give an additional indication of the consistency in the calculations.*

[K] The entropy balance is

$$\frac{\partial s}{\partial t} + \nabla \cdot \mathbf{J}_s + \Gamma_s = \sigma \quad (i)$$

where  $s$  is the entropy,  $t$  is time,  $J_s$  is the entropy current,  $\Gamma_s$  is the entropy source/sink, and  $\sigma$  is the internal entropy production of the macroscopic domain (always positive).

In our case, the divergence of the entropy current can be expanded as follows

$$\frac{\partial s}{\partial t} + \frac{\mu}{T}(\nabla \cdot \mathbf{J}) + \mathbf{J} \cdot \left( \nabla \frac{\mu}{T} \right) + \Gamma_s = \sigma \quad (\text{ii})$$

where  $\mu$  is the chemical potential,  $J$  is the flux at the macroscopic scale.

Applying equation (ii) over one full cycle with a periodic source/sink leads to the temporally integrated form with  $ds/dt = 0$  indicated by the overbar

$$\overline{\frac{\mu}{T}(\nabla \cdot \mathbf{J}) + \mathbf{J} \cdot \left( \nabla \frac{\mu}{T} \right) + \Gamma_s} = \overline{\sigma} \quad (\text{iii})$$

In equation (iii), at the microscopic scale, the entropy production and source/sink term at the land surface, because of evaporation/infiltration, can be expanded as follows

$$\overline{\frac{\mu}{T}(\nabla \cdot \mathbf{J}) + \mathbf{J} \cdot \left( \nabla \frac{\mu}{T} \right) + \sum_i \gamma_i \left( \frac{\mu_\gamma}{T} \right)} = \overline{\sum_i F_i J_i} \quad (\text{iv})$$

where  $F_i$  and  $J_i$  are the microscale forces and fluxes; and  $\gamma_i$  is the strength of the local sources/sinks, and  $\mu_\gamma$  is the chemical potential of the sources/sinks. Thus, equation (iv) incorporates two scales: the divergence of the entropy current at the macroscale (first two terms), and the sources/sinks and entropy production at the microscale (remaining two terms).

In order to explicitly resolve the microscale terms, the hillslope is discretized at the microscale using the uniform grid of ParFlow (finite control volumes with two-point flux approximation). The fluxes in the domain are calculated based on Richards equation at isothermal conditions. Thus, the chemical potential is the hydraulic head (though I stick to  $\mu$  here). The time series of sources/sinks (i.e. infiltration/evaporation) are obtained from the coupling with CLM, which calculates soil moisture dependent evaporation based on the Monin-Obukhov similarity principle.

Additionally, the first macroscopic term on the left hand side can be expanded to

$$\overline{\frac{\mu}{T}(\nabla \cdot \mathbf{J})} = \overline{\sum_i \left( \frac{\mu}{T} \right)_i (\nabla \cdot \mathbf{J})_i} \quad (\text{v})$$

where the divergence of the entropy current due to the divergence of the flux is calculated over individual grid cells and integrated over the full domain i.e. the hillslope (or the subdomains i.e. the recharge and discharge zones).

This part of the divergence, which can be positive or negative locally, was the variable to be plotted in figure 2 and may show different patterns based on the local dynamics of the hillslope and the periodic sources/sinks. In my opinion, these patterns reflect, which parts of the domain act as effective entropy exporters or importers. At dynamic equilibrium over one complete cycle, the periodic entropy sources/sinks are balanced by (1) the microscale entropy production (right hand side of equation (iv)), (2) the macroscale chemical potential and divergence of the flux (first term left hand side of equation (iv)), and a mean

macroscale gradient and flux across the hillslope (second term left hand side of equation (iv))

$$\overline{J \cdot \left( \nabla \frac{\mu}{T} \right)} \neq 0 \quad (\text{vi})$$

because of

$$\overline{\sum_i \gamma_{in,i} \left( \frac{\mu_\gamma}{T} \right)_i} > \overline{\sum_i \gamma_{out,i} \left( \frac{\mu_\gamma}{T} \right)_i} \quad (\text{vii})$$

where  $\gamma_{in,i}$  and  $\gamma_{out,i}$  are the periodic infiltration and exfiltration fluxes at grid cell  $i$ , respectively.

This is proposed to be exploited in the upscaling of a macroscopic force across the hillslope and ultimately the derivation of an effective exchange coefficient. The complete entropy balance calculation is ongoing, and the expanded and revised theory and analysis will be included in the revisions of the manuscript.

[S ] *Secondly, the author presents the mere existence of a maximum in power with varying conductance as indication that “power is indeed maximized” in the simulations. For this statement to be substantiated, it would be necessary to demonstrate that the conductivity resulting in maximum power is indeed the one a hillslope naturally assumes. This has not been done and hence all that could be concluded from this study is that maxima exist along the range of simulated conductivities. In this context, I am uncertain how to interpret the deduced “effective” conductivity and the fact that only one maximum in power is expressed over the range of calculated effective conductivities.*

[K] I agree that the maximum in power has only been shown along a range of simulated conductivities. No connection to reality has been established at this point. This will be clearly stated in the revised manuscript. Based on the comments of all Referees and the additional calculations performed so far, the analysis needs to be revised, the relationships need to be re-established including the interpretation of the results.

[S] *According to P. 5137 L4, the author calculates the effective conductivity as the ratio of average power to the square of average hydraulic head difference. This derivation seems flawed, as the mean of a ratio is not equal to the ratio of two means, and the mean of a square is not equal to the square of a mean. For a correct calculation, the variances and covariances of the variables need to be considered.*

[K] I calculated the effective force from the ratio of the average power to the flux, and with this force in hand I calculated the effective conductivity from the ratio of the average flux to the force.

[S] *I also failed to see the merit of deducing effective conductances and pressure heads from the numerical simulations, given that both of these vary in space and time. I think that derivation of effective static soil properties and effective hillslope or catchment geometry would be more useful. Or, even better, if a global optimum in  $K_{sat}$  with respect to macroscopic power or entropy production exists, it would be very interesting to assess if real hillslopes tend towards such an optimal value.*

[K] I agree that relating a global optimum  $K_{sat}$  with respect to macroscopic power to a real hillslope and deriving static soil properties would be extremely useful. I felt that the derivation of effective conductances and forces is a useful step in this direction.

[S] *I hope that these and the below step-by-step comments will help to improve the manuscript and make it an inspiring and useful addition to the scientific literature.*

[K] I would like to thank the Referee again for his useful comments and suggestions

[S] *1. Throughout: The use of the term optimization is confusing. Entropy production is maximized by optimization of some system properties such as effective conductance or spatial arrangement. If entropy production were to be optimized, as stated in this manuscript, I would expect that something else was the objective function to be maximized or minimized, while entropy production was the adjustable lever. On P5125L3 the term “entropy production optimization (EPO)” is introduced. How does this differ from “maximum entropy production (MEP)”?*

[K] I agree that the term optimization is used inconsistently. This will be clarified in the revised manuscript. The idea of introducing the term entropy production optimization was, because apparently there is still debate about minimization and maximization of entropy production in natural systems.

[S] *2. Throughout: It would be helpful to remind the reader every now and then what the different abbreviations mean, e.g. S1 and S2 being homogeneous or heterogeneous  $K_{sat}$  respectively.*

[K] The suggestion will be honored in the revised manuscript.

[S] *3. Throughout: Please do not use the word “chaos” when referring to heterogeneity. Chaos has a specific mathematical definition and could confuse readers.*

[K] The suggestion will be honored in the revised manuscript.

[S] *4. P5124L13: inference tool*

[K] This will be corrected in the revised manuscript.

[S] 5. P5125L10: *The property of being well mixed or not is unrelated to being stationary or non-linear. To avoid confusion, this section should be re-written and a discussion of macroscopic variables could also be added here.*

[K] With well-mixed I mean that there are no internal gradients. This section will be revised.

[S] 6. P5125L15–: *The discussion of entropy production and associated variables is very confusing. What kind of entropy production is maximised, what are relevant system boundaries? The units given here are not consistent: Chemical potential should be energy per mass or per mole, entropy production should be energy per Kelvin per time, power should be energy per time by definition. Using the notation here, energy should be  $ML^2T^{-2}$ , but this is neither reflected in the units of entropy production, nor in the chemical potential or power.*

[K] The internal entropy production of the system (hillslope) is maximized, which is bounded by no-flow conditions along the bottom and vertical faces, and a free surface overland flow boundary condition at the top (that reduces to no-flow under unsaturated conditions, Kollet and Maxwell (2006)). The hillslope exchanges mass with the outside via sources/sinks (infiltration/evaporation), which are calculated by the land surface model CLM. I followed the convention by Westhoff et al. (2104), equation (1), which the Referee coauthored. Following this convention, entropy production has the units  $ML^2T^{-3}K^{-1}$ .

[S] 7. P5126L5: *Clearer formulation: is optimised to maximise P.*

[K] The suggestion will be honored in the revised manuscript.

[S] 8. P5126L14–16: *Kleidon and Schymanski (2008) did not show that entropy is maximised, they hypothesised that this might be the case. I was hoping that the present manuscript would test this hypothesis.*

[K] The statement will be revised in the manuscript.

[S] 9. P5126L24: *Linearity is not needed to use an idealized box model.*

[K] The statement will be revised in the manuscript.

[S] 10. P5127L6–10: *Need to explain what are the state variables that are supposed to be optimised for maximum entropy production or power.*

[K] Optimization will be clarified in the manuscript.

[S] 11. P5127L16: 2D horizontally or vertically?

[K] 2D vertically, which follows from "cross-section of a synthetic hillslope" in the same sentence.

[S] 12. P5128L10–16: A conceptual drawing of the system boundaries and exchange would be helpful here. Why no-flow conditions? Where does the water go? How are the fluxes within the system and across boundaries computed?

[K] A drawing will be provided. No-flow, because a cross-section of a closed basin or symmetric valley with a (dry) stream in the center of the valley was considered. The fluxes are computed with the coupled model ParFlow-CLM, in which Parflow simulates variably saturated subsurface flow and overland flow, and CLM calculates the infiltration/evaporation fluxes at the land surface. Both are coupled via sources/sinks in ParFlow and the soil moisture in the top ten model layers. There are a number of references on this; the most important details will be repeated in the revised manuscript for completeness.

[S] 13. P5128L17: maximum in P (not optimum)

[K] This will be corrected in the revised manuscript.

[S] 14. P5131L16: This implies no drainage, however on P5529L7 it was mentioned that drainage does occur in some simulations.

[K] A single simulation showed minor surface discharge out of the domain. The equation (4) and language will be revised accordingly.

[S] 15. P5131L19: What does it mean that infiltration equals negative evaporation? Why negative?

[K] At dynamic equilibrium, infiltration  $Q_{\text{inf}} = Q$  equals evaporation  $Q_{\text{ev}} = -Q$ . This will be rephrased.

[S] 16. P5133L7–11: Would this stepwise representation of topography lead to an overestimation of power compared to a more smooth representation?

[K] I will perform additional simulations in order to interrogate this question.

*[S] 17. P5133L15–19: I was not able to follow here. I did not see the circulation patterns or understand whether these bands in Fig. 2 have a meaning or are an artefact.*

[K] The circulation refers to figure 1, where a net flow occurs from right to left (from the recharge to the discharge zone), which is expressed in the lateral gradient of  $H$ . The bands are explained at 5133, 5-11.

*[S] 18. P5134L8–9: I see no evidence for the statement that there is some sort of maximization in the critical zone. Figs. 4 and 6 show that there are maxima as  $K_{sat}$  is varied, but the evidence that the hillslope tends towards such states is not given.*

[K] This will be revised in the manuscript.

*[S] 19. P5135L13: These circulation cells sound interesting, but I was not able to see them.*

[K] They are expressed as gradients in  $H$  in figure 1 (color gradients).

*[S] 20. P5135L15: This is interesting. Does a random perturbation generally result in larger effective conductance, then?*

[K] In this presented analysis yes. This must be double checked in the revised analysis.

*[S] 21. P5136L1–3: This has actually been done in Schymanski et al. (2010): A “microscopic” spatially resolved ecohydrological model was transferred into a macroscopic 2-box model with effective parameters, which were optimised using the MEP principle, and the model results turned out to be very similar to the microscopic model simulations. Could this be attempted here as well?*

[K] Yes, this could be attempted here as well in my opinion.

*[S] 22. P5136L22: The equation given here is wrong, as the mean of a quotient is not equal to the quotient of two means. The mean  $H$  is equal to the mean of  $P/q$ , not to the mean of  $P$  divided by the mean of  $q$ , as long as  $P$  and  $q$  are not independent variables. Therefore, the interpretation of these results is likely flawed.*

[K] This will be reconciled in the revised manuscript.

[S] 23. P5137L4: *Again, mean should be calculated as the mean of all values of , not as the mean of P divided by the square of the mean H.*

[K] This will be reconciled in the revised manuscript.

[S] 24. P5137L18–20: *This conclusion seems unjustified. All the figure shows is that there is a maximum but not that the hillslope tends towards such a maximum.*

[K] This will be rephrased in the revised manuscript.

[S] 25. P5138L9–10: *Again, the results do not indicate to me that a hillslope tends towards an MEP state, they just show that there are maxima in power for certain values of saturated hydraulic conductivity.*

[K] This will be rephrased in the revised manuscript.

[S] 26. P5138L20–24: *I don't see the use of deriving "effective gradients in case of known net fluxes". Both fluxes and gradients vary in time, so what would we gain by this?*

[K] For example, if we obtain effective gradients and exchange coefficients that can be related to observable quantities then we may be able to predict net fluxes based on these variables at different scales in the natural system.

[S] 27. P5140L9–11: *It would be interesting to add an entropy balance to these calculations, in order to test whether the theoretical framework is indeed consistent.*

[K] This is already in progress.

[S] 28. Fig. 1: *Why qualitative and not e.g. a logarithmic colour scheme? Surely, the colour scheme does follow some mathematical transformation anyway. What is the meaning of evaporation greater 0 and infiltration lower than 0 for discharge vs. recharge? This distinction did not make any sense to me.*

[K] Hydraulic head may be negative in parts of the domain, therefore no logarithmic transformation. The sign of evaporation and infiltration follows the convention that the flux is positive along the positive z-axis.

[S] 29. Fig. 2: *I had to look twice in the original manuscript to verify that the red bar was not a printout error. It may be good to mention in the caption that this is the actual result, and discuss in the text what caused it. Here, the scale could also be made quantitative.*



[K] The red bar is related to  $\frac{\mu}{T}(\nabla \cdot \mathbf{J})$  in the divergence of the entropy current  $J_s$ , which has been discussed above. More explanation will be provided in the revised manuscript.

[S] 30. *Fig. 6: The arrangement of a-d is different to Fig. 4, while the shape of Fig. 6a is similar to Fig. 4a. Is this coincidence or a mix-up of the axes labels?*

[K] This is a coincidence.

In the following, comments by Referee S. Schymanski are indicated with [S] and replies by the author are indicated by [K].

[S] *I would like to thank the author for the clarifications and additional analysis laid out in his response. I look forward to seeing the new results. Here I would like to re-emphasise the lack of and need for consistency in units. Entropy production can indeed be expressed in units of  $ML^2T^{-3}K^{-1}$ , as done in Westhoff et al. (2014). However, in the present manuscript, on P5125L17, the units are given as  $MT^{-2}K^{-1}$ , i.e.  $L^2T^{-1}$  are missing. Since Eq. 1 in the manuscript is identical to Eq. 1 in Westhoff et al. (2014), and the units of the variables mentioned in Lines 18–19 are also identical, the units for  $\sigma$  in Line 17 are probably just a typographical error. However, the units given for  $P$  in Line 25 are also inconsistent with “power per unit area”, which should be  $MT^{-3}$ , i.e. energy ( $ML^2T^{-2}$ ) per time per area. This is probably because Eq. 2 is missing a  $\rho g$  (see Eq. 6 in Westhoff et al., 2014). Fixing this will probably not change the interpretation of the results (the missing variables are constants), but it will lead to less confusion and help the reader better understand what is being calculated, and how the results relate quantitatively to other results.*

*For the additional equations presented in response to my comments, I would also like to encourage clear statements about the units of each variable. This will help understand the derivations and calculations. For example, if  $s$  and  $J_s$  are expressed per unit surface area, how are the entropy fluxes at the boundaries ( $J_s$ ) related to area? Are they computed per area of the receiving grid cells or the whole projected hillslope area? I would also like to encourage explicit analysis of the entropy transport due to the boundary fluxes, as these largely determine the entropy balance of the system. An inflow of free water (infiltration) could be seen as an outflow of entropy independent of soil moisture (chemical potential of free water), while evaporation could be seen as an inflow of entropy that depends on soil moisture (chemical potential of bound water). There are probably alternative ways of defining consistent entropy balance components, but such explicit consideration of the entropy balance allows for detailed consistency checks of definitions and of the thermodynamic fluxes in the model as I have found while conducting the analysis published in Schymanski et al. (2010).*

[K] Thank you for the note. I fully agree with the Referee that consistency in units is important and helps the reader in the understanding of the theory, results and discussion. Emphasis will be placed in the revised manuscript on this aspect. This will certainly also include details of the entropy balance including the fluxes in out of the domain. I also find that this leads to useful consistency checks at the microscopic and macroscopic scales. In my opinion, this also helps in connecting the different components of the entropy balance in the interpretation of the results.

Unfortunately, the units for the entropy production on 5125, 17 are a typographical error. It is correct that the units of  $P$  on line 25 were normalized by the specific weight of water, which was stated on line 22 in the original manuscript.

1 Inference in hydrology from entropy balance considerations

2

3 Stefan J. Kollet

4

5 IBG-3, Institute for Bio- and Geosciences, Research Centre Jülich, Jülich, Germany

6 Centre for High-Performance Scientific Computing in Terrestrial Systems, Geoverbund ABC/J, Germany

7

8 Correspondence to: S. Kollet (s.kollet@fz-juelich.de)

9

10 **Abstract**

11 In this study, the method of inference of macroscale potentials, forces and exchange coefficients for  
12 variably saturated flow is outlined based on the entropy balance. The theoretical basis of the method of  
13 inference is the explicitly calculation of the internal entropy production from microscale flux-force  
14 relationships using e.g. hyper-resolution variably saturated groundwater flow models. Emphasis is placed  
15 on the two-scale nature of the entropy balance equation that allows incorporating simultaneously  
16 movement equations at the micro- and macroscale. The method is demonstrated with simple hydrologic  
17 cross-sections at steady state and cyclic sources/sinks at dynamic equilibrium, and provides a  
18 thermodynamic point of view of upscaling in variably saturated groundwater flow. The current  
19 limitations in the connection with observable variables and predictive capabilities are discussed, and  
20 some perspectives for future research are provided.

21

22

## 23 Introduction

24 The current earth sciences literature suggests that entropy balance considerations were mainly applied  
25 in the context of optimality and self-organization. This is because theories of optimality and self-  
26 organization are appealing when dealing with complex non-linear systems, because of their apparent  
27 usefulness in interpreting interactions of gradients and fluxes and in quantifying (predicting) systems'  
28 states and uncertainties. In this context, the entropy balance received attention, because of its physics-  
29 based foundation in non-equilibrium thermodynamics and potential connection with information theory  
30 (e.g., Dewar 2003, Koutsoyiannis 2014). The entropy balance appears to be useful in applications to  
31 hydrologic (e.g., Zehe et al. 2013, Ehret et al. 2014), ecohydrologic (e.g., Dewar 2010, Miedziejko and  
32 Kedziora 2014, del Jesus et al. 2012), and atmospheric sciences (e.g., Paillard and Herbert 2013), and in  
33 general to open complex nonlinear thermodynamic systems (Abe and Okuyama 2011).

34 The entropy balance states that in an open system, the change in entropy equals the internal production  
35 of entropy minus the divergence of the entropy current. A dynamic equilibrium or steady state is  
36 obtained, when entropy production inside (due to e.g. flow processes of heat and water) equals the  
37 divergence of the entropy current i.e. the entropy exchange with the outside. Note also, dynamic  
38 equilibrium refers to a state of stationarity in the statistical sense. Optimality of the dynamic equilibrium  
39 may be achieved, because the gradient, which drives the flux and, thus the production of entropy, is  
40 reciprocally depleted by the same flux (Kleidon et al. 2013).

41 In hydrology, the entropy balance has been applied to conceptual problems based on the overarching  
42 rationale that entropy production is maximized (maximum entropy production, MEP) in obtaining a state  
43 of dynamic equilibrium by optimizing the fluxes and gradients in competition via an adjustment of some  
44 (non-)linear exchange coefficient. There have been some studies demonstrating, how entropy  
45 production can be optimized as a function of an exchange coefficient to obtain a system's state at which  
46 entropy production is indeed at its maximum. In hydrology, there are quite a few examples of the

47 application and discussion of the MEP principle (e.g., Ehret et al. 2014, Westhoff et al. 2014, Kleidon and  
48 Schymanski 2008) also in connection with data (e.g., Zehe et al. 2013). However, its validity and  
49 applicability to hydrologic systems is still in question (Westhoff and Zehe 2013).

50  
51 Often the entropy balance has been applied at steady state with simple bucket models, which are well-  
52 mixed (i.e. without internal gradients). For example, Porada et al. (2011) performed a detailed entropy  
53 production analysis of the land surface hydrologic cycle including the shallow vadose zone assuming  
54 vertical equilibrium of the soil bucket model. Applying linear bucket models without considering internal  
55 gradients, Kleidon and Schymanski (2008) showed that if the natural system possesses enough degrees  
56 of freedom, in case of steady state, the system will tend towards a certain exchange coefficient, when  
57 entropy production is maximized. For similar bucket models, Westhoff et al. (2014) demonstrated the  
58 impact of periodic boundary forcing on entropy production, which may result in more than one  
59 maximum for unique values of the exchange coefficient at dynamic equilibrium. Interestingly, these  
60 studies did not calculate the internal entropy production explicitly; entropy production was estimated  
61 indirectly from the exchange with the outside (i.e. the divergence of the entropy current).

62 Schymanski et al. (2010) recognized the potential in explicitly estimating the internal entropy production  
63 using a simple microscale Klausmeier model (Klausmeier 1999), which is based on coupled equations of  
64 moisture and biomass and is able to produce vegetation patterns, in order to optimize effective values of  
65 a simple two-box model. This study highlights an interesting aspect of entropy balance considerations  
66 related to the inference of upscaled effective parameters and state variables to represent subgrid scale  
67 variability in coarse scale (macroscale) models. Thus, ultimately, the appeal of the entropy balance  
68 maybe the inference of upscaled or effective exchange coefficients and forces/gradients, which may be  
69 used to quantitatively describe the complex system without the explicit knowledge about microscopic  
70 details (Dewar 2009). In this context, a popular example is gas diffusion, which can be captured by an

71 inferred, macroscopic diffusion coefficient and gradient instead of honoring the motion and interactions  
72 of individual molecules.

73 In this study, the method of inference of effective hydrologic exchange coefficients, potentials and forces  
74 is outlined using the entropy balance equation in applications to simple hydrologic cross-sections. The  
75 following sections provide the basic theory with an emphasis on the two-scale nature of the entropy  
76 balance, and the application to the hydrologic cross-sections with ensuing discussion and conclusions.

77

### 78 **Basic theory and the two-scale nature of the entropy balance**

79 The theory outlined in Kondepudi and Prigogine (2015) is applied to the problem of variably saturated  
80 groundwater flow at constant temperature. Based on conservation of energy (and the balance equation  
81 for concentrations, which is not required in this analysis) Kondepudi and Prigogine (2015) write the  
82 entropy balance as follows

$$83 \quad s' + \nabla \cdot J_s = \sigma \quad (1),$$

84 where  $s'$  ( $\text{ML}^{-1}\text{T}^{-3}\text{K}^{-1}$ ) is the change in the entropy density with time;  $J_s$  ( $\text{MT}^{-3}\text{K}^{-1}$ ) is the entropy current per  
85 unit volume; and  $\sigma$  ( $\text{ML}^{-1}\text{T}^{-3}\text{K}^{-1}$ ) is the internal entropy production per unit volume, which is always  
86 positive by definition. Thus, the change of entropy density with time of a macroscopic volume depends  
87 on the divergence of the entropy current and the internal entropy production.

88 In the considered case of variably saturated groundwater flow,  $J_s = JM/T$ , where  $J$  ( $\text{ML}^{-2}\text{T}^{-1}$ ) is the mass  
89 flow per unit area,  $M$  ( $\text{L}^2\text{T}^{-2}$ ) is the chemical potential at the macroscale and  $T$  (K) is the temperature.

90 Defining  $q$  ( $\text{ML}^{-3}\text{T}^{-1}$ ) and  $f$  ( $\text{L}^2\text{T}^{-2}$ ) as the fluxes and forces at the microscale per unit volume, the  
91 divergence of the entropy current and the internal entropy production can be expanded as follows

$$92 \quad s' + (M/T)(\nabla \cdot J) + J \cdot (\nabla(M/T)) = \sum qf/T \quad (2).$$

93 Equation (2) exhibits the unique characteristics of incorporating two scales: the entropy density change  
94 with time and divergence of the entropy current at the macroscale (all terms on the left hand side), and  
95 the entropy production at the microscale i.e. the sum of all products of the internal microscopic fluxes  
96 and forces (term on the right hand side). Note, in the following,  $T(K)$  is omitted in the equations and  
97 units, because  $T = \text{constant}$  in the following derivations.

98 Performing an entropy balance at true steady state leads to

$$99 \quad M(\nabla \cdot J) + J \cdot (\nabla M) = \sigma \quad (3)$$

100 because  $s' = 0$ . In contrast, performing an entropy balance under the influence of periodic external  
101 forcing requires integration over one full forcing cycle at dynamic equilibrium of equation 2 indicated by  
102 overbars

$$103 \quad \overline{M(\nabla \cdot J)} + \overline{J \cdot (\nabla M)} = \overline{\sigma} \quad (4).$$

104 with  $\overline{s'} = 0$  over one full cycle. Both approaches will be applied in the following section, in order to  
105 arrive at effective variables at the macroscale.

106 In order to further emphasize the two-scale nature of equations 1 and 2, movement equations are  
107 introduced at the macro- and microscale. At the macroscale,  $M(L^2T^{-2})$  is defined as the sum of the  
108 macroscopic pressure potential  $\Psi (L^2T^{-2})$ , and gravitational potential  $gz(L^2T^{-2})$ , leading to

$$109 \quad M = \Psi + gz \quad (5);$$

110 and is, thus, equivalent to the hydraulic head;  $(\nabla M)$  symbolizes a macroscopic force  $F(L^2T^{-2})$  being the  
111 difference in the macroscopic chemical potentials

$$112 \quad (\nabla M) = F = M_{high} - M_{low} \quad (6);$$

113 and, at the moment,  $J$  is defined as a conductance concept

114  $J = \lambda F$  (7),

115 where  $\lambda$  ( $\text{ML}^{-4}\text{T}$ ) is a conductance coefficient ( $\lambda = \rho r_s$ , with water density  $\rho$  ( $\text{ML}^{-3}$ ) and resistance  $r_s$  ( $\text{TL}^{-1}$ ))  
116 relating the flux with the force at the macroscale.

117 At the microscale, the chemical potential  $\mu$ , ( $\text{L}^2\text{T}^{-2}$ ), the mass flux  $q$  ( $\text{ML}^{-3}\text{T}^{-1}$ ) per unit volume and the  
118 force  $f$  ( $\text{L}^2\text{T}^{-2}$ ) are

119  $\mu = \psi + gz$  (8),

120 where  $\psi$  ( $\text{L}^2\text{T}^{-2}$ ) is the microscale pressure potential;

121  $q = \frac{1}{\alpha} \rho \frac{K}{\nu} k_r(\psi) (\mu_{high} - \mu_{low})$  (9),

122 where  $\rho$  ( $\text{ML}^{-3}$ ) is the density;  $\nu$  ( $\text{L}^2\text{T}^{-1}$ ) is the kinematic viscosity;  $K$  is the permeability ( $\text{L}^2$ ),  $k_r(\psi)$  (-) is the  
123 relative permeability, and  $\alpha$  ( $\text{L}^{-2}$ ) is the unit microscopic flow through area; and the microscale force

124  $f = (\mu_{high} - \mu_{low})$  (10).

125 Technically,  $\sum qf$  is the sum of all fluxes and forces (both always positive, because any flux produces  
126 entropy) between all neighboring cells or elements in a microscale, numerical, variably saturated  
127 groundwater flow model including any Dirichlet and Neumann boundary conditions.

128 Thus, the two-scale nature of equation 2 allows to apply different flux-force relationships at the different  
129 scales that are the conductance concept at the macroscale (equation 7) and essentially Darcy's law or  
130 Richards equation (equation 7) at the microscale. In equation 2, the entropy production serves as an  
131 "automatic" spatial and also temporal integrator of the microscale fluctuations. These two  
132 characteristics are remarkable. Note, the calculation (integration) of the entropy balance may be  
133 performed over the global domain of volume  $V$  ( $\text{L}^3$ ) or any subdomain  $V_i$  ( $\text{L}^3$ ) thereof.

134



135 **Method of Inference**

136 The basis of the method of inference is that the internal, microscopic entropy production  $\sigma$  and also the  
137 complete entropy balance can be calculated from support scale simulations by implementing the  
138 microscale equations 9 and 10 in combination with a continuity equation over the macroscopic domain.  
139 In obtaining  $\sigma$  explicitly, one is able to estimate effective potentials, forces and conductance coefficients,  
140 at the macroscale (equation 7) from the explicitly resolved fluctuations at the microscale, which are  
141 thermodynamically consistent. In order to illustrate the method of inference of macroscale potentials,  
142 conductances and forces, a number of illustrative examples based on simple hydrologic profiles are  
143 presented applying different boundary conditions and source terms.

144

145 *Example 1:*

146 Directed at a heat flow example in Kondepudi and Prigogine (2015), a simple cross-section is considered  
147 (figure 1) with steady-state, variably saturated groundwater flow,  $J$ , from left to right due to Dirichlet  
148 boundary conditions on the left  $M_l$  and right  $M_r$ , with  $M_l > M_r$ . Because  $\nabla \cdot J = 0$ , and  $s' = 0$  at steady  
149 state, integration of the entropy balance over the cross-section leads to

150 
$$S'_i = \int_0^{L_z} \int_0^{L_x} \sigma(x, z) dx dz = L_z \int_0^{L_x} J_x (\nabla_x M) dx \quad (11a)$$

151 
$$S'_i = L_z J_x (M_l - M_r) = L_z J_x F \quad (11b),$$

152 where  $L_z$  and  $L_x$  (L) are the constant vertical and horizontal extents of the cross-section, respectively;  $S'_i$   
153 is the total internal entropy production; and  $F = (M_l - M_r)$  is the macroscopic force. Note, in the  
154 following, the entropy production integral is simply written as  $S'_i = \int \sigma$ , and  $L_z$  is lumped into the flux  
155  $L_z J_x = J$  for convenience.

156 In case of this simple example, applying  $J = \lambda(M_l - M_r)$  from equation 5, one obtains the expression for  
157 the effective conductance

$$158 \lambda = S'_i(M_l - M_r)^{-2} = S'_i F^{-2} \quad (12)$$

159 and the effective force

$$160 F = S'_i J^{-1} \quad (13).$$

161 Thus, one may obtain the true, effective conductance for any kind of heterogeneity (i.e. microscale  
162 fluctuations) by explicitly calculating  $\sigma$  and  $S'_i$  based on equations 6 and 7 and the macroscopic  
163 boundary conditions  $M_l$  and  $M_r$ . Note, entropy production is simply the sum of the product of the steady  
164 state fluxes and incremental forces over the cross-section

165  $S'_i = \int \sigma = \int (\sum qf) = \int \left( \sum \frac{1}{\alpha} \rho \frac{K}{v} k_r(\psi) (\mu_{high} - \mu_{low})^2 \right)$ , where individual values of  $qf$  are calculated  
166 with equations 9 and 10 between two adjacent microscale elements in support scale numerical  
167 simulations.

168

169 *Example 2:*

170 This example expands example 1 to steady state groundwater flow including recharge represented by  
171 the mass rate  $Q_s$

$$172 Q_s = \int_0^L (\nabla \cdot J) dx \quad (14),$$

173 and integration leading to

$$174 MQ_s + J_l M_l - J_r M_r = S'_i \quad (15).$$

175 where  $M$  is the macroscopic potential of the cross-section.

176 The general expression for the macroscopic potential of the cross-section is

$$177 \quad M = Q_s^{-1}(S'_i - (J_l M_l - J_r M_r)) \quad (16).$$

178 In this example, three special cases are considered, namely  $J_l = 0$ ,  $J_l < 0$ , and  $J_l > 0$ . In case of  $J_l = 0$

179 (figure 2), there is a no-flow boundary condition on the left side resulting in  $J_r = Q_s$  and, thus

$$180 \quad M = S'_{i,J_l=0} Q_s^{-1} + M_r \quad (17)$$

$$181 \quad F = (M - M_r) = S'_{i,J_l=0} Q_s^{-1} \quad (18)$$

182 where the subscript indicates the respective case for the left boundary flux.

183 With equation 7 and  $J_r = Q_s = J$  follows for the conductance coefficient

$$184 \quad \lambda = S'_{i,J_l=0} F^{-2} \quad (19).$$

185 For  $J_l < 0$  (figure 3), the symmetric case is considered, where the potentials at the boundaries are equal

186 ( $M_l = M_r = M_b$ ) and  $Q_s$  is uniform over the profile ( $-J_l = J_r = Q_s/2$ ) leading to

$$187 \quad M Q_s - 1/2 Q_s M_l - 1/2 Q_s M_r = S'_{i,J_l < 0} \quad (20a).$$

$$188 \quad Q_s (M - (M_l + M_r)/2) = S'_{i,J_l < 0} \quad (20b).$$

$$189 \quad Q_s (M - M_b) = S'_{i,J_l < 0} \quad (20c)$$

190 and ultimately for the macroscopic potential

$$191 \quad M = S'_{i,J_l < 0} Q_s^{-1} + M_b \quad (21).$$

$$192 \quad F = (M - M_b) = S'_{i,J_l < 0} Q_s^{-1} \quad (22)$$

193 and

194  $\lambda = S'_{i,J_l < 0} F^{-2}$  (23)

195 Note,  $M$  and  $F$  reflect values for each of the two half-spaces separated by a no-flow boundary condition

196 e.g.  $F = (S'_{i,J_l < 0}/2)(Q_s/2)^{-1}$ , which is true for a homogeneous profile only and is equivalent to the case

197  $J_l < 0$  above. The entropy production is calculated also with

198  $S'_{i,J_l < 0} = \int \sigma = \int (\sum qf) = \int \left( \sum \frac{1}{\alpha} \rho \frac{K}{v} k_r(\psi) (\mu_{high} - \mu_{low})^2 \right).$

199 For a heterogeneous profile and/or  $M_l > M_r$  (figure 4) i.e. when there is no symmetry

200  $MQ_s - J_l M_l - J_r M_r = S'_{i,J_l < 0}$  (24).

201 Thus, the effective potential of the cross section may be obtained from

202  $M = Q_s^{-1} (S'_{i,J_l < 0} + J_l M_l + J_r M_r)$  (25)

203 Additionally, expressions can be obtained for the conductance coefficients in the exchange with the left

204 and right boundary conditions that are

205  $\lambda_l = (MQ_s - S'_{i,J_l < 0} - J_r M_r)(F_l M_l)^{-1}$  (26a)

206  $\lambda_r = (MQ_s - S'_{i,J_l < 0} - J_l M_l)(F_r M_r)^{-1}$  (26b).

207 where the macroscale forces  $F_r = M - M_r$  and  $F_l = M - M_l$  result from the differences between  $M$  and

208  $M_l, M_r$  with  $M$  following from equation 25. Again, entropy production is calculated with

209  $S'_{i,J_l < 0} = \int \sigma = \int (\sum qf) = \int \left( \sum \frac{1}{\alpha} \rho \frac{K}{v} k_r(\psi) (\mu_{high} - \mu_{low})^2 \right).$

210 For  $J_l > 0$  (figure 5), the entropy balance is

211  $MQ_s + J_l M_l - J_r M_r = S'_{i,J_l > 0}$  (27)

212 and the macroscopic potential is

213  $M = Q_s^{-1}(S'_{i,J_l>0} - J_l M_l + J_r M_r)$  (28)

214 With  $Q_s = J_r - J_l$  follows

215  $J_l(M_l - M) + J_r(M - M_r) = S'_{i,J_l>0}$  (29)

216 Thus, two conductances can be obtained, which are

217  $\lambda_l = (S'_{i,J_l>0} - J_r(M - M_r)) F_l^{-2}$  (30)

218  $\lambda_r = (S'_{i,J_l>0} - J_l(M_l - M)) F_r^{-2}$  (31)

219 with the macroscopic forces  $F_l = (M_l - M)$  and  $F_r = (M - M_r)$ . In this example, two additional

220 conductances can be obtained for the subdomains separated by the dividing streamline due to recharge

221 shown in figure 5 that are

222  $\lambda_{Q_s} = (S'_{i,J_l>0} - J_l(M_l - M_r)) F_{Q_s}^{-2}$  (32)

223  $\lambda_{l,r} = (S'_{i,J_l>0} - Q_s(M - M_r)) F_{l,r}^{-2}$  (33)

224 with  $J_r = J_l + Q_s$ , and the macroscale forces  $F_{Q_s} = (M - M_r)$  and  $F_{l,r} = (M_l - M_r)$ . In the domain, the

225 entropy production is calculated also with

226  $S'_{i,J_l>0} = \int \sigma = \int (\sum qf) = \int \left( \sum \frac{1}{\alpha} \rho \frac{K}{v} k_r(\psi) (\mu_{high} - \mu_{low})^2 \right).$

227

228 **Example 3:**

229 In this example, a no-flow boundary condition on the left is considered resembling a hillslope with a no-

230 flow boundary along a hypothetical ridge on the left side, and a Dirichlet boundary condition along a

231 hypothetical stream on the right side. Now, a source/sink  $Q_s(x,t)$  varies periodically in space and time

232 (periodically varying recharge/discharge). In this case, equation 2 needs to be solved for the different  
 233 variables and integrated over one complete cycle at dynamic equilibrium.

234 Note, again  $\int_0^L \nabla \cdot J dx = Q_s$ , because there is a macroscopic, transient source/sink in the domain,  
 235 therefore, after integration along the cross-section, the entropy balance reads

$$236 \quad S' + M Q_s - J_r M_r = S'_i \quad (34)$$

237 where  $S'$  is the entropy change rate. After time integration over one full cycle at dynamic equilibrium,  
 238  $\overline{Q_s} = 0$  and  $\overline{S'} = 0$ , the effective macroscopic potential of the cross-section due to the periodic varying  
 239 source/sink is

$$240 \quad \overline{M} = \overline{(S'_i + J_r M_r - S')} Q_s^{-1} \quad (35a)$$

241 or

$$242 \quad \overline{M} = \text{cov}(S'_i, Q_s^{-1}) + \overline{S'_i} \overline{Q_s^{-1}} + M_r (\text{cov}(J_r, Q_s^{-1}) + \overline{J_r} \overline{Q_s^{-1}}) + \text{cov}(S', Q_s^{-1}) \quad (35b)$$

243 Recognizing that  $J_r = \int_0^L (Q_s - \theta') dx$ , where  $\theta'$  is the macroscopic mass change rate of the cross-  
 244 section, one obtains for the effective force

$$245 \quad \overline{F} = \overline{(S'_i - \theta' M_r - S')} Q_s^{-1} \quad (36a)$$

246 or

$$247 \quad \overline{F} = \text{cov}(\sigma, Q_s^{-1}) + \overline{\sigma} \overline{Q_s^{-1}} - M_r \text{cov}(\theta', Q_s^{-1}) + \text{cov}(s', Q_s^{-1}) \quad (36b)$$

248 with  $\overline{\theta} = 0$ ; and for the effective conductance

$$249 \quad \overline{\lambda} = \overline{(S'_i - \theta' M - S')} F^2 \quad (37a)$$

250 or

251 
$$\bar{\lambda} = \text{cov}(S'_i, F^2) + \overline{S'_i F^2} - \text{cov}(\Theta' M, F^2) + \overline{\Theta' M F^2} + \text{cov}(S', F^2) \quad (37b)$$

252 with  $J_r = \lambda F = \lambda(M - M_r)$ .

253 Apparently, on the right hand side of equations 35, 36, and 37 all terms may be calculated from the  
 254 numerical simulations except  $S' = \int s'$  and therefore also  $\text{cov}(S', Q_s^{-1})$ , because  $S'$  and  $M$  is not known  
 255 in equation 34 (note,  $S'_i$  is calculated explicitly). However,  $S'$  may actually be calculated from the  
 256 microscale variables, which is demonstrated with a discrete example depicted in the schematic in  
 257 figure 6.

258 In this schematic, there are three microscale elements with sources/sinks in each individual element ( $q_b$ ,  
 259  $q_c$ ,  $q_r$ ) and a constant potential boundary condition on the right ( $\mu_b$ ). For each individual element the  
 260 entropy balance is

261 
$$s'_l + q_l \mu_l - q_{l,c} \mu_{l,c} = \sum q_l f_l = q_{l,c} (\mu_l - \mu_{l,c}) \quad (38a)$$

262 
$$s'_c + q_c \mu_c + q_{l,c} \mu_{l,c} - q_{c,r} \mu_{c,r} = \sum q_c f_c = q_{l,c} (\mu_{l,c} - \mu_c) + q_{c,r} (\mu_c - \mu_{c,r}) \quad (38b)$$

263 
$$s'_r + q_r \mu_r + q_{c,r} \mu_{c,r} - q_b \mu_b = \sum q_r f_r = q_{c,r} (\mu_{c,r} - \mu_r) + q_b (\mu_r - \mu_b) \quad (38c)$$

264 where the fluxes and potentials with the subscript  $l,c$  and  $c,r$  are valid at the element interfaces. The  
 265 terms on the right hand side i.e. the entropy production for each element encompass the fluctuations in  
 266 the flux-force relationships between the element's interior and the element boundaries. Summation of  
 267 the individual balance equations leads to the total balance

268 
$$s' + q_l \mu_l + q_c \mu_c + q_r \mu_r - q_b \mu_b = \sigma = q_{l,c} (\mu_l - \mu_c) + q_{c,r} (\mu_c - \mu_r) + q_b (\mu_r - \mu_b) \quad (39).$$

269 Note, on the left hand side, all the interface terms disappear and only the source and boundary terms  
 270 remain, equivalent to the macroscale balance in equation 34. Equation 38 is the entropy balance  
 271 equation for the system depicted in figure 6.

272 Any changes in the entropy of the system with time are due to transient effects that cancel out at  
 273 dynamic equilibrium  $\bar{s}' = 0$ . In order to demonstrate this, substitution of  $q_{l,c} = (q_l - \theta'_l)$ ,  $q_{c,r} =$   
 274  $(q_l - \theta'_l) + (q_c - \theta'_c)$ , and  $q_b = (q_l - \theta'_l) + (q_c - \theta'_c) + (q_r - \theta'_r)$  for the interface fluxes on the right  
 275 hand side in equation 38 leads to

$$s' + q_l \mu_l + q_c \mu_c + q_r \mu_r - q_b \mu_b =$$

$$276 (q_l - \theta'_l) \mu_l + (q_c - \theta'_c) \mu_c + (q_r - \theta'_r) \mu_r - q_b \mu_b \quad (40)$$

277 which demonstrates continuity in case of true steady state  $\theta'_l = \theta'_c = \theta'_r = 0$ , and shows that any e.g.  
 278 positive mass storage change  $\theta'$  over the microscopic volume leads to negative change in entropy and  
 279 vice versa. Note, the entropy production is still always positive. Thus,  $S'$  and can be evaluated by  
 280 applying equation 39 to microscale simulations.

281 A special case may be considered, in which the system depicted in figure 6 is also closed on the right side  
 282 resulting in a sole exchange with the surroundings via the periodic source/sink  $Q_s(t)$ . This would be  
 283 equivalent to a profile with a discharge area in the center and the assumption of symmetry shown in the  
 284 schematic in figure 7. The requirement again is that  $\bar{Q}_s = 0$  over one full cycle at dynamic equilibrium.  
 285 Then e.g. equation 35 simplifies to

$$286 \bar{M} = \overline{(S'_l - S')} Q_s^{-1} \quad (41a)$$

287 or

$$288 \bar{M} = \text{cov}(\Delta S', Q_s^{-1}) + \overline{S'_l Q_s^{-1}} \quad (41a)$$

289 with  $\Delta S' = S'_l - S'$ .

290

291



292 **Discussion**

293 The major advantage of the proposed inference theory is the estimation of macroscopic variables that  
294 are thermodynamically consistent with the microscale fluctuations. This is discussed in the context of the  
295 simple example 1 interpreting the entropy current  $J_s = JM$  as an advective potential flux. Because  $J$  is  
296 constant and  $M_l > M_r$ , the entropy current leaving the domain on the right side is smaller than the  
297 entropy current entering the domain on the left side. This is due to dissipation in the interior of the  
298 domain resulting into the production of entropy  $S'_i$ . In hydrology, the dissipation is simulated using  
299 Darcy's law and Richards equation at the support (here microscopic) scale, where all dissipative  
300 processes are lumped in the hydraulic conductivity representing the flow resistance. Thus, at the  
301 macroscale the derived conductance  $\lambda$  is thermodynamically consistent if one accepts e.g., Darcy's law as  
302 a valid parameterization of the internal dissipative processes.

303 Equations 12 and 13 have not been applied before in the context of hydrology. While the equations  
304 illustrate the basic idea for the simplest case of a Darcy experiment, one may argue that the insight  
305 gained from this example is rather limited, because  $\lambda$  could have been obtained from the known flux-  
306 force relationship and the conductance equation (one unknown  $\lambda$  with one equation 7). Examples 2 and  
307 3, on the other hand, clearly illustrate the advantage, because the macroscale potential  $M$  (and  
308 therefore  $F$ ), which are needed to obtain  $\lambda$  are not known in these examples. Thus, one is left with two  
309 unknowns  $\lambda$  and  $F$ , and only one equation (the conductance equation 7). In the proposed theory, the  
310 entropy balance provides the second equation to solve for the two unknowns at the cost of explicitly  
311 calculating the internal entropy production  $S'_i = \int \sigma = \int (\sum_{\alpha} \frac{1}{\alpha} \rho \frac{K}{v} k_r(\psi) (\mu_{high} - \mu_{low})^2)$ ,  
312 and at the benefit of thermodynamic consistency. This is the central message of the proposed method of  
313 inference, which utilizes  $S'_i$  as a spatial and also temporal integrator.

314 It is important to emphasize that one can also obtain, in an ad hoc fashion, the forces and conductance  
315 coefficients for any sub-domain  $V_i$  of the global domain with volume  $V$ . For example, in order to obtain  
316 the macroscale potential in the center of the profile of example 1, one arrives at

$$317 \quad M_c = M_l - J^{-1} \int_{V_i} \sigma dV_i \quad (42).$$

318 Thus, from  $\int_{V_i} \sigma dV_i$  estimates, one is able to obtain macroscale variables over a hierarchy of scales for  
319 different hydrologic configurations similar to the simple examples provided above.

320 Under purely saturated groundwater flow conditions, the estimates of macroscale variables can be used  
321 directly for predictions, because  $\lambda$  is constant for the same flow geometries, which is trivial, but  
322 important to realize. In case of variably saturated flow and transient conditions (when the flow geometry  
323 changes),  $\lambda$  is of course not constant and  $S'_i$  will depend in an unknown, non-linearly fashion on the flux  $J$   
324 and its variability (example 3), which apparently limits the usefulness of the proposed approach.

325 However, universal relationships of  $S'_i(J)$  and  $\text{cov}(S'_i, J^{-1})$  can perhaps be obtained from a series of  
326 numerical experiments under characteristic hydrologic configurations.

327 This also brings up the question, whether one is able to establish a connection of the proposed theory  
328 with observations of real-world systems. Obviously,  $S'_i$  and  $S'$  can not be measured directly in the field  
329 utilizing independent experiments, which could, in turn, be used to derive macroscopic forces from flux  
330 observations that are more readily available. Thus, utilizing the entropy balance for estimating  
331 macroscopic field variables and ensuing predictions appears limited at this point. Yet, this study suggests  
332 to explore relationships of measurable field variables and  $S'_i$  utilizing numerical experiments, in future. In  
333 turn, under certain conditions, estimates of  $S'_i$  from measurable quantities may be possible. With the  
334 help of the extended example 1, this is discussed below.

335 Assuming a time varying force i.e. Dirichlet boundary conditions, temporal integration of equation 11  
336 over one full cycle at dynamic equilibrium yields

$$337 \quad \bar{S}'_i = \bar{J}\bar{F} \quad (43)$$

338 Inserting the conductance equation into equation 43 under saturated, linear groundwater flow  
339 conditions with the assumption of only small changes in the flow geometry ( $\lambda$  is constant) leads to

$$340 \quad \bar{S}'_i = \lambda^{-1}\bar{J}^2 = \lambda^{-1}[\text{var}(J) + \bar{J}^2] \quad (44).$$

341 Thus, entropy production is related inversely to  $\lambda$ , linearly with  $J$ , and power two with  $\bar{J}$ . If an estimate  
342 of  $\lambda$  is available,  $\bar{S}'_i$  can be calculated from observations of  $J$ . In the more realistic case of variably  
343 saturated groundwater flow and/or varying flow geometry, equation 44 changes to

$$344 \quad \bar{S}'_i = \overline{\lambda^{-1}J^2} = \text{cov}(\lambda^{-1}, J^2) + \overline{\lambda^{-1}}\bar{J}^2 \quad (45).$$

345 illustrating the same dependence of  $\bar{S}'_i$  on  $\bar{\lambda}$  and  $\bar{J}$  as before. The unknown covariance  $\text{cov}(\lambda^{-1}, J^2)$  may  
346 potentially be estimated from numerical experiments.

347

## 348 **Summary and conclusions**

349 In this study, the method of inference based on the entropy balance equation was introduced. The  
350 theoretical basis is the explicit calculation of the internal microscale entropy production, which is used in  
351 the balance equation to solve for macroscale potentials, forces and fluxes. The proposed method was  
352 illustrated with simple hydrologic cross-sections of steady-state, variably saturated groundwater flow and  
353 a periodic source/sink at dynamic equilibrium.

354 The entropy balance equation is remarkable, because the equation unifies the macro- and microscale in  
355 one equation allowing the simultaneous application of two different movement equations that are the

356 conductance equation at the macroscale and Darcy's law/Richards equation at the microscale, in this  
357 study. The derivations lead to expressions for macroscale variables that are a function of the entropy  
358 production (i.e. the internal fluctuations of the microscale flux-force relationships) and are, thus,  
359 thermodynamically consistent. Therefore, the derivation provides a different theoretical point of view of  
360 variably saturated groundwater flow and new approaches for obtaining effective macroscale variables.  
361 The discussion suggests that these may be derived consistently for a hierarchy of scales. With the advent  
362 of high-performance computing in hydrology, there is strong potential for additional insight from hyper-  
363 resolution numerical experiments to explicitly calculate the internal entropy production. For example,  
364 existing and new averaging and upscaling laws may be tested and derived using series of numerical  
365 experiments with e.g. varying subsurface heterogeneity configurations, and boundary conditions. These  
366 experiments may also be useful in deriving new movement equations at the macroscale replacing  
367 empirical, calibrated parameterizations and regionalization approaches.

368 Thus, the appeal of the proposed method is mainly theoretical at this point, providing a thermodynamics  
369 perspective of inference in hydrology. The connection to real-world observations needs to be established  
370 in future, also with the help of numerical simulations. In the provided theoretical setting, the usefulness  
371 of the method for predictions is evident from the simple examples provide here, however, for real-world  
372 predictions this remains to be demonstrated.

373

#### 374 **References**

- 375 Dewar, R. (2003) Information theory explanation of the fluctuation theorem, maximum entropy  
376 production and self-organized criticality in non-equilibrium stationary states. *Journal of Physics a-*  
377 *Mathematical and General* 36(3), 631-641.
- 378 Koutsoyiannis, D. (2014) Entropy: From Thermodynamics to Hydrology. *Entropy* 16(3), 1287-1314.

379 Zehe, E., Ehret, U., Blume, T., Kleidon, A., Scherer, U. and Westhoff, M. (2013) A thermodynamic  
380 approach to link self-organization, preferential flow and rainfall-runoff behaviour. *Hydrology and Earth  
381 System Sciences* 17(11), 4297-4322.

382 Ehret, U., Gupta, H.V., Sivapalan, M., Weijs, S.V., Schymanski, S.J., Blöschl, G., Gelfan, A.N., Harman, C.,  
383 Kleidon, A., Bogaard, T.A., Wang, D., Wagener, T., Scherer, U., Zehe, E., Bierkens, M.F.P., Di Baldassarre,  
384 G., Parajka, J., van Beek, L.P.H., van Griensven, A., Westhoff, M.C. and Winsemius, H.C. (2014) Advancing  
385 catchment hydrology to deal with predictions under change. *Hydrology and Earth System Sciences* 18(2),  
386 649-671.

387 Dewar, R.C. (2010) Maximum entropy production and plant optimization theories. *Philosophical  
388 Transactions of the Royal Society B-Biological Sciences* 365(1545), 1429-1435.

389 Miedziejko, E.M. and Kedziora, A. (2014) Impact of plant canopy structure on the transport of ecosystem  
390 entropy. *Ecological Modelling* 289, 15-25.

391 del Jesus, M., Foti, R., Rinaldo, A. and Rodriguez-Iturbe, I. (2012) Maximum entropy production, carbon  
392 assimilation, and the spatial organization of vegetation in river basins. *Proceedings of the National  
393 Academy of Sciences of the United States of America* 109(51), 20837-20841.

394 Paillard, D. and Herbert, C. (2013) Maximum Entropy Production and Time Varying Problems: The  
395 Seasonal Cycle in a Conceptual Climate Model. *Entropy* 15(7), 2846-2860.

396 Abe, S. and Okuyama, S. (2011) Similarity between quantum mechanics and thermodynamics: Entropy,  
397 temperature, and Carnot cycle. *Physical Review E* 83(2).

398 Kleidon, A., Zehe, E., Ehret, U. and Scherer, U. (2013) Thermodynamics, maximum power, and the  
399 dynamics of preferential river flow structures at the continental scale. *Hydrology and Earth System  
400 Sciences* 17(1), 225-251.

401 Westhoff, M.C., Zehe, E. and Schymanski, S.J. (2014) Importance of temporal variability for hydrological  
402 predictions based on the maximum entropy production principle. *Geophysical Research Letters* 41(1), 67-  
403 73.

404 Kleidon, A. and Schymanski, S. (2008) Thermodynamics and optimality of the water budget on land: A  
405 review. *Geophysical Research Letters* 35(20).

406 Westhoff, M.C. and Zehe, E. (2013) Maximum entropy production: can it be used to constrain conceptual  
407 hydrological models? *Hydrology and Earth System Sciences* 17(8), 3141-3157.

408 Porada, P., Kleidon, A. and Schymanski, S.J. (2011) Entropy production of soil hydrological processes and  
409 its maximisation. *Earth System Dynamics* 2(2), 179-190.

410 Schymanski, S.J., Kleidon, A., Stieglitz, M. and Narula, J. (2010) Maximum entropy production allows a  
411 simple representation of heterogeneity in semiarid ecosystems. *Philosophical Transactions of the Royal  
412 Society B-Biological Sciences* 365(1545), 1449-1455.

413 Klausmeier, C.A. (1999) Regular and irregular patterns in semiarid vegetation. *Science* 284(5421), 1826-  
414 1828.

415 Dewar, R.C. (2009) Maximum Entropy Production as an Inference Algorithm that Translates Physical  
416 Assumptions into Macroscopic Predictions: Don't Shoot the Messenger. *Entropy* 11(4), 931-944.

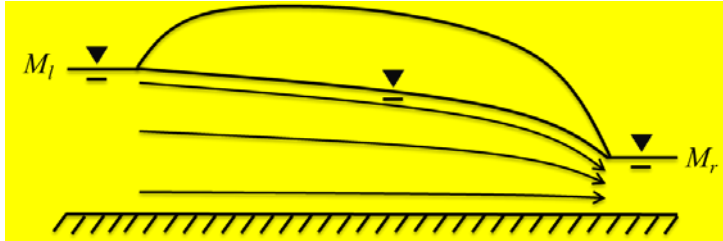
417 Kondepudi, D. and Prigogine, I. (2015) *Modern Thermodynamics: From Heat Engines to Dissipative  
418 Structures, 2nd Edition. Modern Thermodynamics: From Heat Engines to Dissipative Structures, 2nd  
419 Edition, 1-523.*

420

421

422 **Figures**

423



424

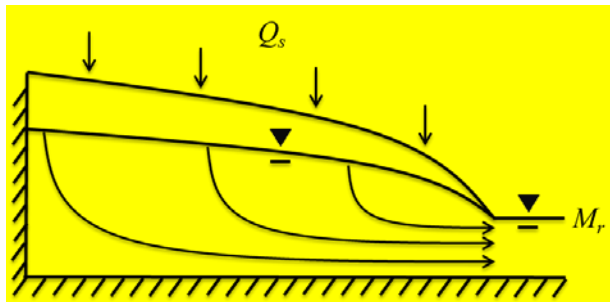
425 Figure 1. Schematic of a simple profile with Dirichlet boundary conditions on the right and left ( $M_r, M_r$ )

426 and steady state variably saturated flow. In the theory, the vertical and horizontal extents of the cross-

427 section are assumed to be constant.

428

429



430

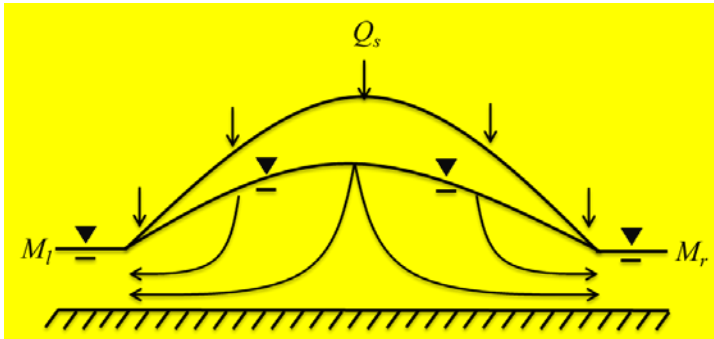
431 Figure 2. Schematic of a simple profile with a Dirichlet boundary condition on the right ( $M_r$ ), a no-flow

432 boundary condition on the left, a constant source ( $Q_s$ ), and steady state variably saturated groundwater

433 flow. In the theory, the vertical and horizontal extents of the cross-section are assumed to be constant.

434

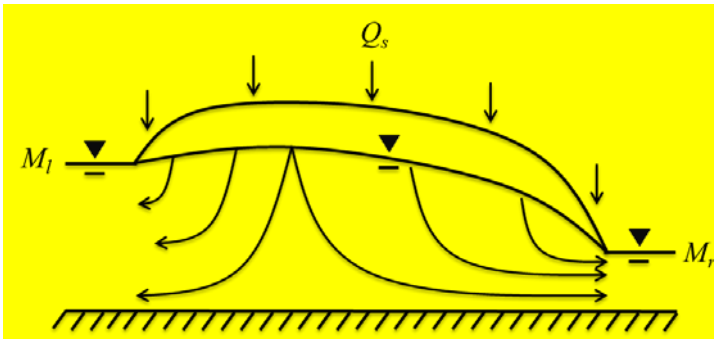
435



436

437 Figure 3. Schematic of a simple profile with Dirichlet boundary conditions on the right and left ( $M_l, M_r$ ) and a  
438 constant source ( $Q_s$ ), and steady state variably saturated groundwater flow. In this symmetric case,  
439 there exist a water divide in the center of the domain. In the theory, the vertical and horizontal extents  
440 of the cross-section are assumed to be constant.

441

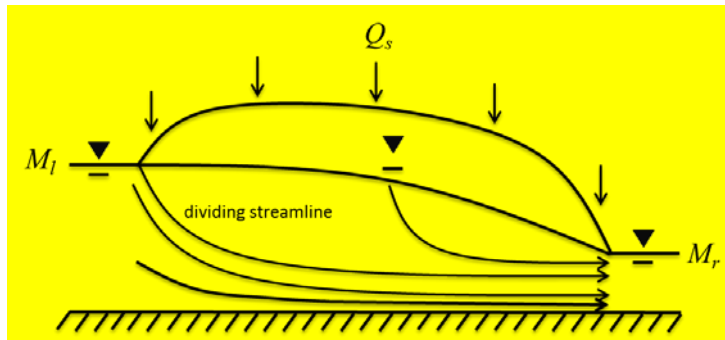


442

443 Figure 4. Schematic of a simple profile with Dirichlet boundary conditions on the right and left ( $M_l, M_r$ ) and a  
444 constant source ( $Q_s$ ), and steady state variably saturated flow. In this case there exist a water divide in  
445 the domain. In the theory, the vertical and horizontal extent of the cross-section is assumed to be  
446 constant.

447





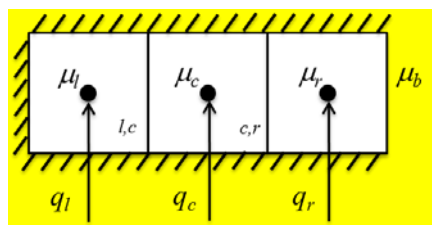
448

449 Figure 5. Schematic of a simple profile with Dirichlet boundary conditions on the right and left ( $M_r, M_l$ ), a  
 450 constant source ( $Q_s$ ), and steady state variably saturated groundwater flow. Note the dividing streamline  
 451 in this example. In the theory, the vertical and horizontal extents of the cross-section are assumed to be  
 452 constant.

453

454

455

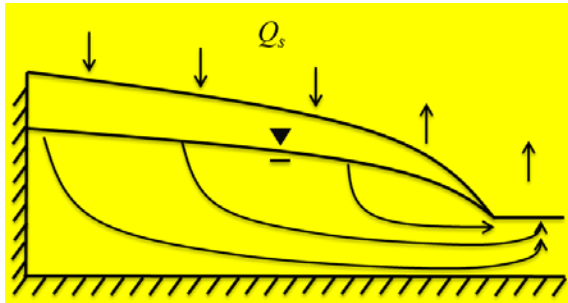


456

457 Figure 6. Schematic of the discrete example consisting of three microscale elements with a Dirichlet  
 458 boundary condition on the right side ( $\mu_b$ ) and a source/sink in each element ( $q_l, q_c, q_r$ ).

459

460



461

462 Figure 7. Schematic of a simple profile with a no-flow boundary condition on the left and right (based on

463 symmetry) and transient, spatially varying sources/sinks  $Q_s(x, t)$  resulting in a recharge and discharge

464 area. In the theory, the vertical and horizontal extent of the cross-section is assumed to be constant.

465